Evidence of antimagnetic rotation in odd-A ^{105}Cd

Deepika Choudhury,[1,*] A. K. Jain,[1] M. Patial,[1] N. Gupta,[1] P. Arumugam,[1] A. Dhal,[2,6] R. K. Sinha,[2] L. Chaturvedi,[3]
P. K. Joshi,[4] T. Trivedi,[4] R. Palit,[4] S. Kumar,[5] R. Garg,[5] S. Mandal,[5] D. Negi,[6] G. Mohanto,[6] S. Muralithar,[6] R. P. Singh,[6]
N. Madhavan,[6] R. K. Bhowmik,[6] and S. C. Pancholi[6]

[1]*Department of Physics, Indian Institute of Technology, Roorkee 247667, India*
[2]*Department of Physics, Banaras Hindu University, Varanasi 221005, India*
[3]*Department of Pure and Applied Physics, Guru Ghasidas University, Bilaspur 495009, India*
[4]*Department of Nuclear and Atomic Physics, Tata Institute of Fundamental Research, Mumbai 400085, India*
[5]*Department of Physics and Astrophysics, University of Delhi, Delhi 110007, India*
[6]*Inter University Accelerator Center, New Delhi 110067, India*

The lifetimes of the levels above spin $23/2^-$ in the negative-parity yrast band of ^{105}Cd have been measured using the Doppler shift attenuation method. The obtained $B(E2)$ values are small and show a decrease with an increase in spin. This establishes, for the first time, antimagnetic rotation (AMR) in an odd-A nucleus. An excellent agreement between the theoretical (semiclassical model) and experimental results along with a large $\Im^{(2)}/B(E2)$ ratio for the states strongly suggests that the structure of the levels beyond spin $23/2^-$ has the character of a twin-shears type AMR band resulting from the coupling of a pair of $g_{9/2}$ proton holes with aligned $h_{11/2}$ and $(g_{7/2})^2$ neutron particles, along with a small contribution from the core rotation.

Observation of a regular pattern of γ rays in nearly spherical Pb nuclei in the early 1990s [1,2] opened a new era in high-spin physics. Unlike the normal deformed and superdeformed rotational bands, these rotationlike bands, now known as magnetic rotation (MR) bands, are predominantly $M1$ in nature with very weak or absent crossover $E2$ transitions. The data table compiled by Amita *et al.* in 2000 [3], and further revised in 2007 [3], contains 178 MR bands in 76 nuclides distributed in $A = 80$, 110, 135, and 190 regions. Frauendorf [4,5] proposed what is now known as "the shears mechanism" of generation of angular momentum in these bands.

In analogy to antiferromagnetism in solids, Frauendorf also proposed [5] an alternative arrangement of the proton and neutron angular momentum vectors ($\vec{j}_\pi$ and $\vec{j}_\nu$), which also breaks the symmetry about the total angular momentum vector $\vec{I}$. This may lead to a new kind of phenomenon termed "antimagnetic rotation" (AMR) where two pairs of nucleons in a twin-shears configuration are aligned back to back. In the $A = 110$ region, a pair of proton angular momentum vectors (arising due to a pair of proton holes in high-Ω $g_{9/2}$ orbitals) are in a stretched mode with the neutron spin vector (arising due to high-j low-Ω neutron particle configuration) in the middle and nearly perpendicular to both of them (see Fig. 1). Generation of higher angular momenta is by the simultaneous closing of the two proton blades toward the direction of $\vec{I}$. Since $\vec{\mu}_\perp$ of the two subsystems are antialigned and cancel each other, there is no net magnetic dipole moment. As the system is symmetric with respect to a rotation of π around the axis of $\vec{j}_\nu$ or $\vec{I}$, the levels in the AMR band differ in spin by $2\hbar$ and are connected by weak $E2$ transitions reflecting a small deformation of the nucleus.

The experimental data on AMR are very scarce and tentative in nature. The only firm evidence of AMR was reported in the positive-parity yrast bands in ^{106,108}Cd [6–8], although tentative claims do exist for the occurrence of this phenomenon in some other nuclei such as ^{100}Pd, ^{109,110}Cd, and ^{144}Dy [9–11]. However, there is no confirmed case of an AMR band in an odd-A nucleus so far.

In the present work, we focus on the odd-A ^{105}Cd nucleus, the level scheme of which has been studied earlier by Regan *et al.* [12] in 1993 and by Jerrestam *et al.* [13] in 1995. We have measured the lifetimes ($\lesssim 1$ ps) of the states above spin $23/2^-$ in the negative-parity yrast band by using the Doppler shift attenuation method (DSAM). The measured lifetimes are found to be in conformity with the characteristic features of AMR. Further, calculations based on an extended version of the semiclassical model [11,14] confirm the AMR nature of the band in ^{105}Cd. In addition to showing that AMR is possible in an odd-A nucleus, the present work opens the possibility of finding AMR in odd-A nuclei in other mass regions.

Excited states of ^{105}Cd nuclei were populated by the ^{94}Zr(^{16}O,$5n$) reaction at a beam energy of 93 MeV. The ^{16}O beam was delivered by the 15-UD Pelletron accelerator at the Inter University Accelerator Centre (IUAC), New Delhi. An isotopically enriched ^{94}Zr target of thickness 1.35 mg/cm^2 on ^{197}Au backing of thickness 8.86 mg/cm^2 was used for the experiment. The deexciting γ rays were detected by using the Indian National Gamma Array (INGA) [15] comprising 14 Compton suppressed clover detectors arranged in five rings (at 32°, 57°, 90°, 123°, and 148° with respect to the beam direction). A total of 1.2×10^9 γ-γ coincidences were collected. The coincidence events were sorted into the traditional $4k \times 4k$ E_γ-E_γ symmetric matrices and angle-dependent asymmetric matrices using the INGASORT [16] analysis program. The symmetric matrices were used in the RADWARE program [17] for coincidence analysis.
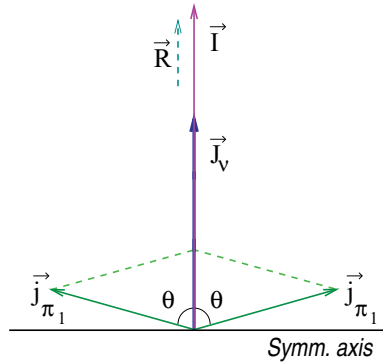
*deepika.chry@gmail.com

FIG. 1. (Color online) Coupling of angular momentum of the proton blades ($\vec{j}_{\pi_1}$ and $\vec{j}_{\pi_2}$ at a dynamic angle of 2θ to each other) and the neutron blade ($\vec{J}_\nu$). The total angular momentum $\vec{I} = \vec{I}_{\rm sh} + \vec{R}$ where $\vec{R}$ is due to core rotation and $\vec{I}_{\rm sh}$ is the sum of $\vec{j}_{\pi_1}$, $\vec{j}_{\pi_2}$ and $\vec{J}_\nu$.

FIG. 3. Sum gated coincidence spectrum showing the in-band and side-feeding transitions in the negative-parity yrast band.

A partial level scheme of ^{105}Cd relevant to the present work is shown in Fig. 2. The energies, intensities, and multipolarities of transitions obtained from the present data mostly agree with the earlier published works [12,13] with two exceptions: (1) energies of the $43/2^- \rightarrow 39/2^-$ and $47/2^- \rightarrow 43/2^-$ transitions are observed to be 1462 and 1581 keV, respectively,
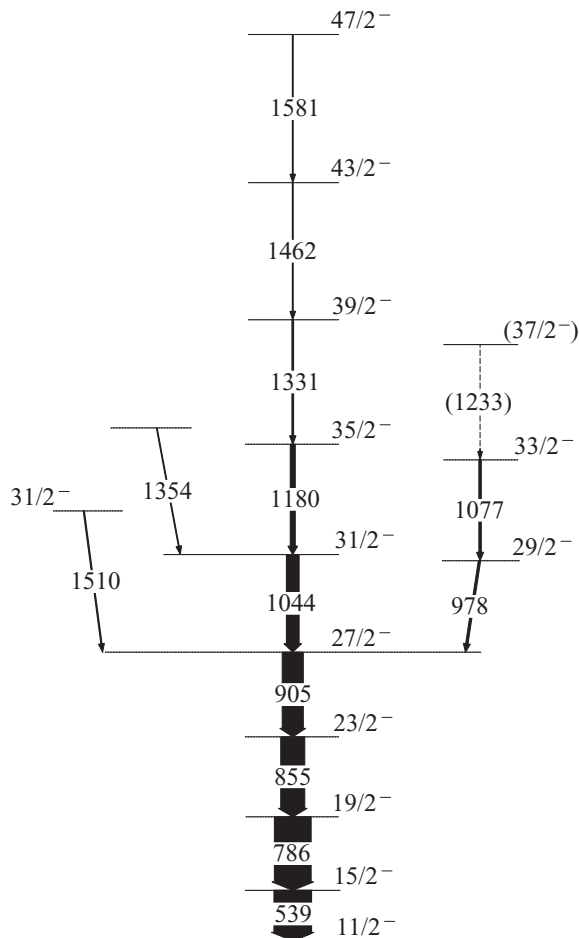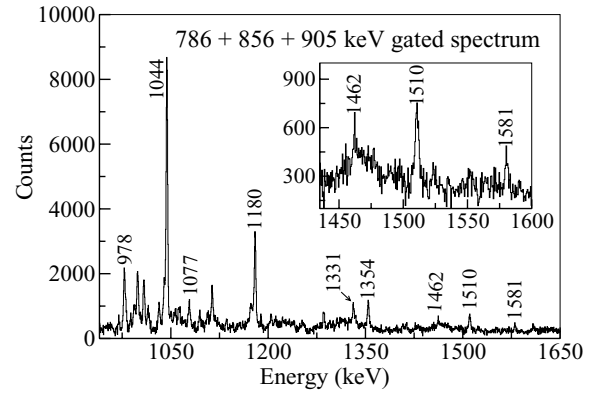
and (2) no evidence is found for the 1443-keV transition, decaying from $41/2^- \rightarrow 37/2^-$, reported earlier. The sum gated coincidence spectrum, with gates on 786-, 855-, and 905-keV transitions, shown in Fig. 3 confirms these findings. Table I lists the properties of the negative-parity states and the connecting transitions as obtained from the present work.

Using the angle-dependent asymmetric matrices (all vs $32°$, all vs $90°$, and all vs $148°$), lifetimes of the states in the negative-parity yrast band of ^{105}Cd were extracted by fitting the Doppler broadened line shapes of the γ-ray energies by using the LINESHAPE analysis code of Wells and Johnson [18]. Simulating the slowing down of the recoiling nuclei in the target and backing, a velocity profile for the recoil was generated by using Monte Carlo methods with a time step of 0.001 ps for 5000 histories of energy losses at different depths. These profiles were generated for groups of detectors at angles of $32°$, $90°$, and $148°$, incorporating the clover geometry of the detectors. For calculating the energy losses, the electronic stopping powers of Northcliffe and Schilling [19] corrected for shell effects have been used. The energies of the decaying γ rays and the intensities of the side feedings

FIG. 2. Partial level scheme of ^{105}Cd.

TABLE I. Energies, relative intensities, and DCO ratios (with gate on 539.3-keV transition energy) for the transitions among the negative-parity states of ^{105}Cd.

E_γ (keV)	E_i (keV)	I_γ	$R_{\rm DCO}$	$I_i^\pi (\hbar)$	$I_f^\pi (\hbar)$
539.3	1702.3	100	–	$15/2^-$	$11/2^-$
785.5	2487.8	97.8(22)	0.94(6)	$19/2^-$	$15/2^-$
855.2	3343.0	64.0(13)	0.99(8)	$23/2^-$	$19/2^-$
905.0	4248.0	56.3(10)	0.97(8)	$27/2^-$	$23/2^-$
977.8	5225.8	9.5(9)	–	$29/2^-$	$27/2^-$
1043.7	5291.7	33.9(8)	0.96(12)	$31/2^-$	$27/2^-$
1077.2	6303.0	6.4(8)	1.09(25)	$33/2^-$	$29/2^-$
1179.6	6471.3	13.3(7)	1.12(22)	$35/2^-$	$31/2^-$
1331.0	7802.3	4.4(5)	0.89(25)	$39/2^-$	$35/2^-$
1354.1	6645.8	3.9(5)	–	–	$31/2^-$
1461.8	9264.1	2.4(3)	–	$43/2^-$	$39/2^-$
1510.4	5758.4	3.1(4)	–	$31/2^-$	$27/2^-$
1580.5	10844.6	2.2(4)	–	$47/2^-$	$43/2^-$

into the states were used as input parameters for line shape analysis. The side feeding into each level of the band was considered as a cascade of five transitions having a fixed moment of inertia comparable to that of the in-band sequences. Assuming 100% side feeding into the top of the band, an effective lifetime of the top-most state was estimated which was then used as an input parameter to extract the lifetimes of lower states in the cascade. During each line shape simulation, the background parameters, intensities of the contaminant peaks, and side-feeding quadrupole moments were allowed to vary, and for each set of parameters, the simulated line shapes were fitted to the experimental spectra using the χ^2 minimization routines of MINUIT [20]. After minimizing the χ^2 values for each state individually, a global fit of the full cascade was performed to deduce the lifetime of each of the states. Using the MINOS routine [20], the uncertainty in the lifetimes were determined from the vicinity of the minimum. Figure 4 shows the line shape fits for the transition energies of 1044 and 1180 keV, decaying from $31/2^-$ and $35/2^-$ states, respectively, for the extreme forward ($32°$), transverse ($90°$), and extreme backward ($148°$) angle gated spectra with the gate set on the 539 keV ($15/2^- \rightarrow 11/2^-$) transition.

Due to lack of statistics in the forward angle ($32°$) spectra, lifetimes of states above $35/2^-$ were determined by using only the backward angle ($148°$) gated spectra. Figure 5 shows the line shape fits for the representative transition energies 1331 and 1462 keV decaying from states $39/2^-$ and $43/2^-$, respectively. The deduced lifetimes (τ) and reduced transition

FIG. 5. (Color online) Representative spectra (with gate on the 539-keV transition) along with theoretically fitted line shapes for 1331 and 1462 keV transition energies in the negative-parity yrast band of ^{105}Cd for γ-ray spectra at $148°$ with respect to the beam direction.

probability $B(E2)$ values along with their respective fitting errors are shown in Table II. The obtained $B(E2)$ values are found to decrease with an increase in spin. The dynamic moment of inertia $\Im^{(2)}$ has been found to be nearly constant (~25–$30\hbar^2$ MeV^{-1}) as a function of rotational frequency $\hbar\omega$ [see insert in Fig. 7].

The negative-parity yrast band of ^{105}Cd is built upon a single $\nu(h_{11/2})$ neutron from the $[550]1/2^-$ Nilsson orbital [12,13]. The first band crossing is observed at a rotational frequency of ~0.43 MeV which has been interpreted to be due to the alignment of a pair of $g_{7/2}$ neutrons [12,13], thus assigning the $\nu[h_{11/2}(g_{7/2})^2]$ configuration to this band above $I = 23/2$. The three-neutron configuration, represented by a combined neutron angular momentum vector $\vec{J}_\nu$, is subsequently coupled to a pair of $g_{9/2}$ proton holes, each represented by $\vec{j}_\pi$ such that at $I \sim 23/2$ each of the two proton angular momentum vectors are pointing opposite to each other and are nearly perpendicular to the neutron angular momentum vector, $\vec{J}_\nu$ (see Fig. 1). Beyond spin 23/2, the angular momentum generation is by the gradual alignment of the two $g_{9/2}$ proton hole angular momentum vectors $\vec{j}_\pi$ toward the neutron angular momentum vector $\vec{J}_\nu$, that is, by the closing of twin shears along with a small contribution from the slightly deformed core. Because of the symmetry of the configuration, the rotation axis coincides with one of the principal axes.

Macchiavelli *et al.* [14,21] had devised a semiclassical particle plus rotor model to study the competition between shears mechanism and core rotation in magnetic rotation
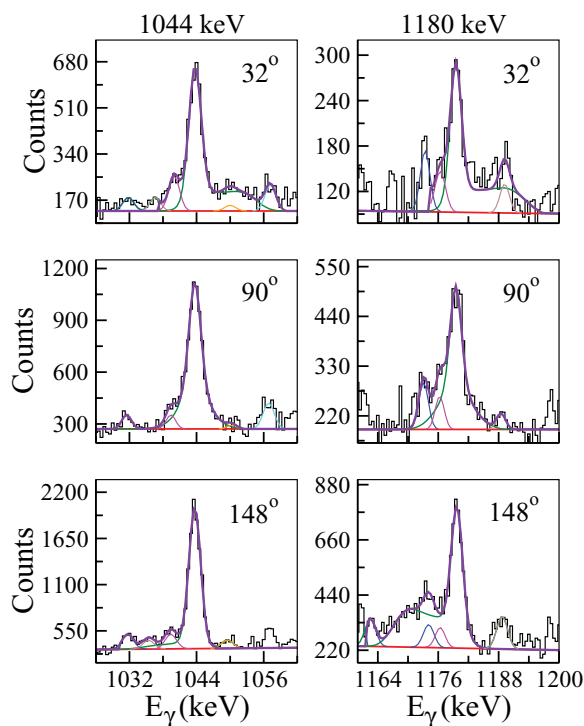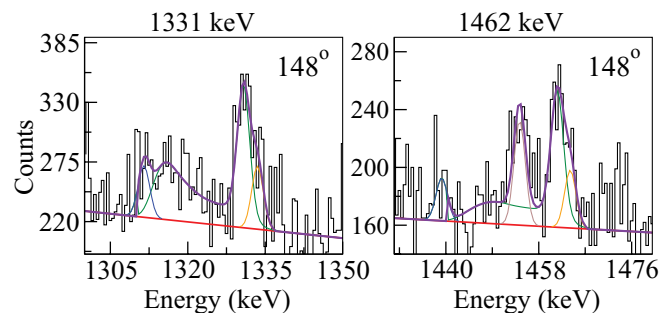

FIG. 4. (Color online) Representative spectra (with gate on the 539-keV transition) along with theoretically fitted line shapes for 1044- and 1180-keV transition energies in the negative-parity yrast band of ^{105}Cd for γ-ray spectra at $32°$, $90°$, and $148°$ with respect to the beam direction.

TABLE II. Results of the line shape analysis for ^{105}Cd. τ represents the mean lifetime of the state (I_i^π) deexciting by a γ ray of energy E_γ. $B(E2)$ is the corresponding reduced transition probability.

$I_i^\pi \rightarrow I_f^\pi (\hbar)$	E_γ (keV)	τ (ps)	$B(E2)$ $(e\,\text{b})^2$
$27/2^- \rightarrow 23/2^-$	905.0	$1.066^{+0.141}_{-0.102}$	$0.126^{+0.012}_{-0.017}$
$31/2^- \rightarrow 27/2^-$	1043.7	$0.621^{+0.082}_{-0.082}$	$0.106^{+0.082}_{-0.082}$
$35/2^- \rightarrow 31/2^-$	1179.6	$0.399^{+0.045}_{-0.031}$	$0.089^{+0.007}_{-0.010}$
$39/2^- \rightarrow 35/2^-$	1331.0	$0.207^{+0.031}_{-0.029}$	$0.094^{+0.013}_{-0.014}$
$43/2^- \rightarrow 39/2^-$	1461.8	$0.237^{+0.046}_{-0.049}$	$0.052^{+0.011}_{-0.010}$

bands. The model was extended by Sugawara *et al.* [11] to include both magnetic and antimagnetic rotation for a four-quasiparticle configuration comprising two high-j protons and two high-j neutrons. The total energy was expressed as the sum of the rotational energy of the core and effective interactions of the form $V_2 P_2 \cos(\theta)$ between the blades. In the model, magnitudes of each proton and neutron vector blade were assumed to be the same, that is, $|\vec{j}_\pi| = |\vec{j}_\nu|$. In the present work, we have extended the semiclassical model by considering $|\vec{j}_\pi| \neq |\vec{j}_\nu|$. Here we consider the coupling of three neutrons (particles) and two protons (holes). The total energy is given by

$$E(I) = \frac{(I - \vec{j}_{\pi_1} - \vec{j}_{\pi_2} - \vec{J}_\nu)^2}{2\Im} + V\left(\frac{3\cos^2\theta - 1}{2}\right) - \frac{V}{6}\left(\frac{3\cos^2(2\theta) - 3}{2}\right), \quad (1)$$

where $\Im$ is the moment of inertia of the core. The effective interaction for each pair (either particle-particle or particle-hole) has been assumed to be identical in magnitude and equal to $\frac{V}{6}$. The sign of V is negative for particle-particle (or hole-hole) interaction and positive for particle-hole interaction, which makes the last term of Eq. (1) negative. There are six possible particle-hole pairs and one possible hole-hole pair. Hence the particle-hole interaction is six times compared to the hole-hole interaction as shown in Eq. (1). By setting $(\frac{dE}{d\theta})_I = 0$ and taking $j_{\pi_1} = j_{\pi_2} = j_\pi$, the expressions for I and ω are obtained as follows:

$$I = \{2j_\pi \cos\theta + J_\nu\} + \frac{3V\Im}{2j_\pi}\cos\theta\left[1 - \frac{2}{3}\cos(2\theta)\right], \quad (2)$$

$$\omega = \frac{3V}{2j_\pi}\cos\theta\left[1 - \frac{2}{3}\cos(2\theta)\right]. \quad (3)$$

The I vs ω values for ^{105}Cd calculated using the semiclassical model (SCM) for spins 23/2 and above is compared with the empirical values (Fig. 6) after adding a constant core contribution of $\omega_o = 0.38$ MeV, which corresponds to the angular momentum contribution in curly brackets in Eq. (2).
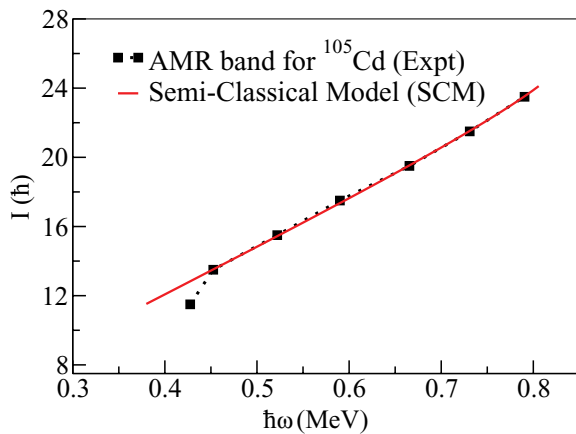

FIG. 6. (Color online) Comparison of the measured I vs ω values from spin 23/2 with those calculated from the semiclassical particle-rotor model (SCM).

An excellent agreement is obtained for $\Im = 19\hbar^2$ MeV^{-1}, $V = 1.92$ MeV, and $J_\nu = 23/2$. This strengthens our interpretation of the aforementioned configuration and that the increase in spin beyond $I = 23/2$ is due to a new type of twin-shears mechanism, that is, AMR. It appears that a minimum value of ω_o is needed to weaken the proton pairing correlations and ready them for the alignment along $\vec{I}$.

In the light of the semiclassical model description, the reduced transition probability, $B(E2)$ can be written as

$$B(E2) = \frac{15}{32\pi}(eQ)_{\text{eff}}^2\left[1 - \left(\frac{I - J_\nu - R}{2j_\pi}\right)^2\right]^2. \quad (4)$$

Here, R represents the contribution from the core rotation.

To compare the behavior of the empirical $B(E2)$ values with the calculated results, we use two methodologies. One is to assume R to be a linear function of angular momentum [22] and express it as $R = (\Delta R/\Delta I)(I - I_b)$, where I_b is the band head spin (=23/2) and $\Delta R/\Delta I = 0.36$ (for the present case). Also, we take $j_\pi = 9/2$, $J_\nu = 23/2$, and $(eQ)_{\text{eff}} = 0.93$ e b [6]. The calculated $B(E2)$ values as a function of spin are shown in Fig. 7(a) along with the experimentally obtained values. Calculations have also been done by using another methodology, that is, first by substituting $R = 2\hbar$ in Eq. (4) (considering that the core rotation contributes a spin of $2\hbar$ beyond $I = 23/2$) and then by substituting $R = 4\hbar$ (considering $4\hbar$ core contribution from spin 39/2). The calculated and experimental $B(E2)$ vs I values are compared in Fig. 7(b). Whereas the first method assumes a linear increase in core rotation, the second method assumes
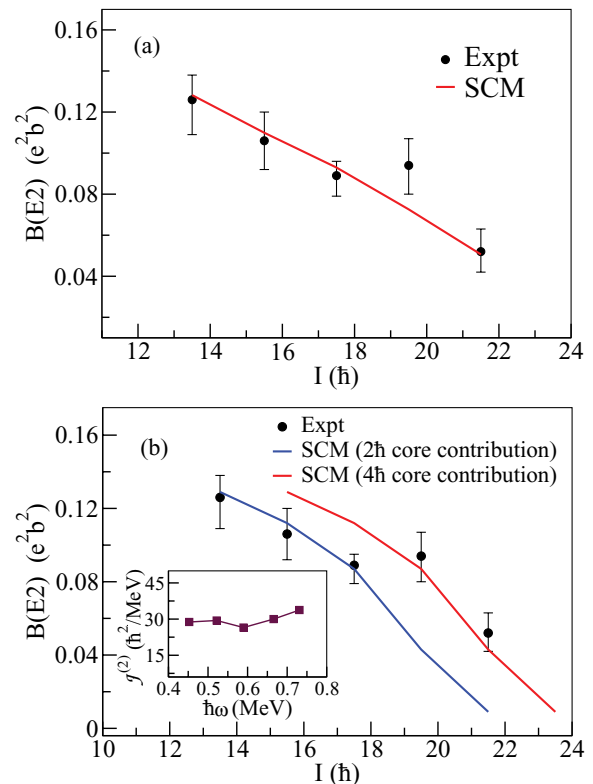

FIG. 7. (Color online) Comparison of experimentally obtained $B(E2)$ vs I for the negative-parity yrast band of ^{105}Cd.

a quantum jump in core rotation from $2\hbar$ to $4\hbar$ at $I = 39/2$ and better reproduces the sudden change in the experimental $B(E2)$ values after $I = 35/2$. The sudden change in $B(E2)$ is matched by a small dip at $I = 35/2$ in the plot of $\Im^{(2)}$ vs $\hbar\omega$ [insert of Fig. 7(b)].

To summarize, we have measured the lifetimes of the high-spin states (above $23/2^-$) in the yrast band of ^{105}Cd by using the DSAM and $B(E2)$ values have been extracted. The decreasing trend in the experimentally obtained $B(E2)$ values with increase in spin has been interpreted by using a semiclassical model. Generation of high-spin states beyond spin $23/2^-$ occurs due to the gradual closing of the proton vectors toward the aligned neutron vectors along with a small contribution from the core rotation. The observed

small $B(E2)$ values [$\sim$0.05–0.13 $(e$ b$)^2$] decreasing with increasing spin along with constant $\Im^{(2)}$ ($\sim$30 $\hbar^2$ MeV^{-1}) and large $\Im^{(2)}/B(E2)$ ratio [$>$150 $\hbar^2$ MeV^{-1} $(e$ b$)^{-2}$] increasing with spin establish that the band is an example of the new kind of twin-shears mechanism. This is the first definitive result indicating that the AMR is operative in an odd-A nucleus.

[1] H. Hübel *et al.*, Prog. Part. Nucl. Phys. **28**, 427 (1992).
[2] R. M. Clark *et al.*, Phys. Lett. B **275**, 247 (1992).
[3] Amita, A. K. Jain, and B. Singh, At. Data Nucl. Data Tables **74**, 283 (2000), revised edition at [http://www.nndc.bnl.gov/publications/preprints/mag-dip-rot-bands.pdf].
[4] S. Frauendorf, Nucl. Phys. A **557**, 259 (1993).
[5] S. Frauendorf, Rev. Mod. Phys. **73**, 463 (2001).
[6] A. J. Simons *et al.*, Phys. Rev. Lett. **91**, 162501 (2003).
[7] A. J. Simons *et al.*, Phys. Rev. C **72**, 024318 (2005).
[8] P. Datta *et al.*, Phys. Rev. C **71**, 041305 (2005).
[9] S. Zhu *et al.*, Phys. Rev. C **64**, 041302(R) (2001).
[10] C. J. Chiara *et al.*, Phys. Rev. C **61**, 034318 (2000).
[11] M. Sugawara *et al.*, Phys. Rev. C **79**, 064321 (2009).
[12] P. H. Regan *et al.*, J. Phys. G **19**, L157 (1993).
[13] D. Jerrestam *et al.*, Nucl. Phys. A **593**, 162 (1995).
[14] R. M. Clark and A. O. Macchiavelli, Annu. Rev. Nucl. Part. Sci. **50**, 1 (2000).
[15] S. Muralithar *et al.*, Nucl. Instrum. Methods Phys. Res. Sect. A **622**, 281 (2010).
[16] R. K. Bhowmik, S. Muralithar, and R. P. Singh, DAE Symp. Nucl. Phys. B **44**, 422 (2001).
[17] D. C. Radford, Nucl. Instrum. Methods A **361**, 297 (1995).
[18] J. C. Wells and N. R. Johnson, ORNL Physics Division Progress, Report No. ORNL-6689, p. 44 (1991).
[19] L. C. Northcliffe and R. F. Schilling, Nucl. Data Tables **7**, 233 (1970).
[20] F. James and M. Roos, Comput. Phys. Commun. **10**, 343 (1975).
[21] A. O. Macchiavelli *et al.*, Phys. Rev. C **57**, R1073 (1998); **58**, 3746 (1998).
[22] R. M. Clark *et al.*, Phys. Rev. Lett. **82**, 3220 (1999).